A 9-DoF Wheelchair-Mounted Robotic Arm System: Design, Control, Brain-Computer Interfacing, and Testing

Redwan Alqasemi and Rajiv Dubey
University of South Florida
Tampa, Florida
USA

1. Introduction

A wheelchair-mounted robotic arm (WMRA) system was designed and built to meet the needs of mobility-impaired persons with limitations of upper extremities, and to exceed the capabilities of current devices of this type. The control of this 9-DoF system expands on the conventional control methods and combines the 7-DoF robotic arm control with the 2-DoF power wheelchair control. The 3-degrees of redundancy are optimized to effectively perform activities of daily living (ADLs) and combine wheelchair mobility and arm manipulation to overcome singularities, joint limits and some workspace limitations. The control system is designed for teleoperated or autonomous coordinated Cartesian control, and it offers expandability for future research. Several interchangeable user interfaces were implemented in the design, including a Brain Computer Interface (BCI). That BCI system was modified and integrated to the control of the WMRA system for users who are totally paralyzed or "locked-in" and cannot use conventional augmentative technologies, all of which require some measure of muscle control. Testing and data collection were performed on human subjects, and the design, various optimized control methods and test results are presented in this paper.

According to the 2006 US Census Bureau report (US Census Bureau, 2002), about 51.2 million Americans (18.1 percent of the US population) had some level of disability and 32.5 million of them (11.5 percent) had a severe disability. About 10.7 million Americans older than 6 years of age needed personal assistance with one or more activities of daily living (ADL). This work focuses on people who have limited or no upper extremity mobility due to spinal cord injury or dysfunction, or genetic predispositions, or people who are "locked-in" (e.g., by end-stage amyotrophic lateral sclerosis, brainstem stroke, or severe polyneuropathy). Robotic aides used in these applications may vary from advanced limb orthosis to robotic arms (Reswick, 1990).

A wheelchair mounted robotic arm can enhance the manipulation capabilities of individuals with disabilities that are using power wheelchairs, and reduce dependence on human aides.

Unfortunately, most WMRAs have had limited commercial success due to poor usability and low payload. It is often difficult to accomplish many of the Activities of Daily Living (ADL) tasks with the two commercial WMRAs currently on the market due to its physical and control limitations. Furthermore, the lack of the integration of the robotic arm controller with the wheelchair controller leads to an increased mental load on the user. This project attempts to surpass available commercial WMRA devices by offering an intelligent system that combines the mobility of the wheelchair and the manipulation of a newly designed arm in an effort to improve performance, usability, control and reduce mental burden on the user while maintaining cost competitiveness.

It is desired to fulfill the need of such integrated systems to be used for many ADL tasks such as opening a spring-loaded door autonomously and going through it, interactively exchange objects with a companion on the move, and avoiding singularities in a small working environment, such as an office, where wheelchair motion can be slightly utilized to maneuver objects while avoiding singularities (similar to a person sitting on an office chair and handling surrounding objects by moving his/her arm while slightly moving the chair to get closer to an object that is otherwise unreachable). These tasks can be performed without the need to switch between the wheelchair controller and the robotic arm controller. The implementation of the combined control will still give the user the option to control the robotic arm alone or the wheelchair alone.

In addition, a Brain-Computer Interface (BCI), which does not require any muscular activity for device manipulation, is also a feasible control mechanism for the totally paralyzed users. For a "locked-in" user, the BCI control system introduces a wide range of self-performed ADL tasks that are otherwise impossible to perform independently.

2. Background

There are several designs of workstation-based robotic arm systems, but WMRAs combine the idea of workstation and mobile-base robots to mount a manipulator arm onto a power wheelchair. One of the most important design considerations of where to mount a robotic arm in a power wheelchair is the safety of the operator (Yanco, 1998). There have been several attempts in the past to create commercially viable wheelchair mounted robotic arms, including the two currently available WMRAs: Manus and Raptor.

The Manus manipulator, manufactured by Exact Dynamics, available since the early 1990s (Eftring & Boschian, 1999), can be programmed in a manner comparable to industrial robotic manipulators. A picture of Manus mounted onto a wheelchair is shown in Figure 1. It is a 6 DoF arm, with servomotors all housed in a cylindrical base. Besides the fact that it is controlled independent of the wheelchair control, the current controller allows for Cartesian control, but when it comes close to a singularity, it stops and waits for the user to move it in a different direction. This kind of control increases the cognitive load on the user.

Another production WMRA is the Raptor, manufactured by Applied Resources (Mahoney, 2001), as shown in Figure 2, which mounts to the right side of the wheelchair. This manipulator has four degrees of freedom plus a planar gripper. The user directly controls the arm with either a joystick or a keypad controller. Because the Raptor does not have encoders, the manipulator cannot be controlled in Cartesian coordinates. This compromise was done to minimize the cost, but it decreases the usability of the arm.

Various redundancy resolution methods were developed in the past to optimize a solution based on certain criteria function. Weighted least norm solution method was used by Chan et al (Chan & Dubey, 1995) to penalize the motion of some joints over others. This method can be used in the case of WMRAs to make the wheelchair motion as a secondary motion when needed. The combination of mobility and manipulation has been studied by researchers in the form of a mobile platform that carries a robotic arm. Chung, et al (Chung & Velinsky, 1999) resolved the kinematic redundancy by decomposing the mobile manipulator into two different subsystems, the mobile platform and the manipulator. Each one of these subsystems is controlled independently with an interaction algorithm between the two controllers.

Fig. 1. Manus arm.

Fig. 2. Raptor arm.

Mirosaw (Galicki, 2005) used external penalty functions to enforce the holonomic manipulability and collision avoidance. His results showed continuous velocities near obstacles. An extension to different redundancy resolution schemes has been proposed by

Luca (Luca et al., 2006) to include the representation of mobile platforms in the Jacobian. His simulation showed consistent results.

BCI systems have been used in the past to control peripheral devices such as TVs, cell phones, and computers among others (Farwell & Donchin, 1988). In the case of BCI-controlled computers, the control can be extended to operate rehabilitation devices, prosthetic limbs, and robotic hands. However, using a brain computer interface to control a robotic system is relatively new and primarily at a research stage. In this work, conventional user interfaces, such as a spaceball, a joystick, a keypad and a touch screen, were used to control the WMRA system. A Brain-Computer Interface (BCI) was modified along this line of work and implemented as one of the modular interchangeable user interfaces for the WMRA to be controlled and used by the locked-in patients who are paralyzed from the neck down. This allows the user to communicate action choices to the robot using the BCI.

Farwell and Donchin (Farwell & Donchin, 1988) developed a BCI system that utilized the P300 component of the Event Related Brain Potential (ERP) to allow a locked-in patient to "type" text into a computer without using any neuromuscular function.

D. Valbuena et. al. and T. Lüth et. al. (Valbuena et al., 2007; Lüth et al., 2007) used a Steady-state Visual Evoked Potentials (SSVEP) system to control a semi-autonomous robot to provide a user 1½ hours of independence. The BCI transforms high level orders from the user into low level commands for the robot. The user selects tasks, such as pouring a liquid into a glass, from a menu to control the robotic arm.

The main objective of this work is to develop and optimize a control system that combines the manipulation of the newly designed 7-DoF robotic arm and the mobility of a modified 2-DoF wheelchair in a single control algorithm. Redundancy resolution is to be optimally solved to avoid singularities and joint limits as well as to allow larger wheelchair or manipulator motion depending on the proximity to the goal. The controller is capable of moving autonomously or using teleoperation. A Brain-Computer Interface (BCI) system is to be modified and adapted to the modular control algorithm to allow locked-in users to communicate with the WMRA system and command it to perform a pre-selected list of commands.

3. Motion Control of the 9-DoF WMRA System

3.1 Wheelchair Motion

The differential drive used in power wheelchairs represents a 2-DoF system that moves in plane (Papadopoulos & Poulakakis, 2000). When wheelchair motion control is not combined with the mobile manipulator control, it is always desired to align the wheelchair in certain direction to position the arm in the desired position and orientation to perform ADLs. In this case, non-holonomic constraints on mobile platforms restrict the system's ability to control all 3-DoFs in the workspace. Trajectory planning is required to compensate for the lost DoF in that plane. Suppose that the wheelchair is commanded to move the arm's base reference frame from "T0" position to "T1" position, where "T" is the homogeneous transformation matrix of the corresponding configuration, the motion can be divided into three sub-motions that can be planned in six steps to realize the X-direction motion, Y-direction motion and the Z-direction orientation. The following six steps can be programmed to execute these three sub-motions: First, from the initial point of the arm base at "T0", find the corresponding wheelchair's frame transformation matrix at that pose.

Second, from the destination point of the arm base at "T1", find the corresponding wheelchair's frame transformation matrix at that pose. Third, draw a virtual line between the two new frame transformations of the wheelchair's frame, and find the angle of that line using the transformation resultant between the two. Fourth, command the wheelchair to rotate to the angle of the new line with no translation. Fifth, command the wheelchair to move in a straight line from the initial position to the final position of the wheelchair, ignoring the orientation. Sixth, command the wheelchair to rotate from the angle of the new line to that of the final position. Figure 3 shows the trajectory planning resulting in three sub-motions when given the initial and final position and orientation:
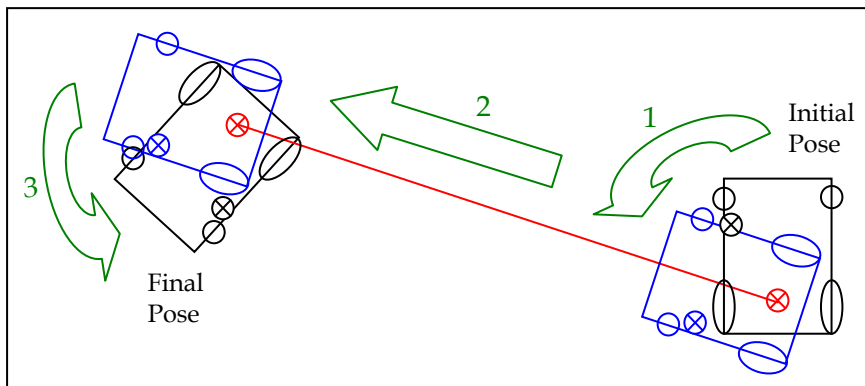
Fig. 3. Trajectory planning for planar motion.

When the wheelchair control is combined with the manipulator control, the above procedure is not necessary since the total system will be redundant. Assuming that the manipulator is mounted on the wheelchair with "L2" and "L3" offset distances from the center of the differential drive across the x and y coordinates respectively (as shown in Figure 4), the mapping of the wheels' velocities to the manipulator's end effector velocities along its coordinates is defined by:

$$\dot{q}_c = J_c \cdot J_W \cdot V_c \tag{1}$$

where:

$$\dot{q}_c = \begin{bmatrix} \dot{x} & \dot{y} & \dot{z} & \dot{\alpha} & \dot{\beta} & \dot{\phi} \end{bmatrix}^T \ , \quad V_c = \begin{bmatrix} \dot{\theta}_l \\ \dot{\theta}_r \end{bmatrix} ,$$

$$J_c = \begin{bmatrix} [I]_{2x2} & \begin{bmatrix} -(P_{xg} \cdot S\phi + P_{yg} \cdot C\phi) \\ P_{xg} \cdot C\phi - P_{yg} \cdot S\phi \end{bmatrix} \\ [0]_{2x2} & [0]_{3x1} \\ [0]_{2x2} & 1 \end{bmatrix}_{6x3} , \text{ and}$$

$$J_W = \frac{L_5}{2}\begin{bmatrix} c\phi_c + \dfrac{2}{L_1}(L_2 s\phi_c + L_3 c\phi_c) & c\phi_c - \dfrac{2}{L_1}(L_2 s\phi_c + L_3 c\phi_c) \\ s\phi_c - \dfrac{2}{L_1}(L_2 c\phi_c - L_3 s\phi_c) & s\phi_c + \dfrac{2}{L_1}(L_2 c\phi_c - L_3 s\phi_c) \\ \dfrac{-2}{L_1} & \dfrac{2}{L_1} \end{bmatrix}_{3x2}$$
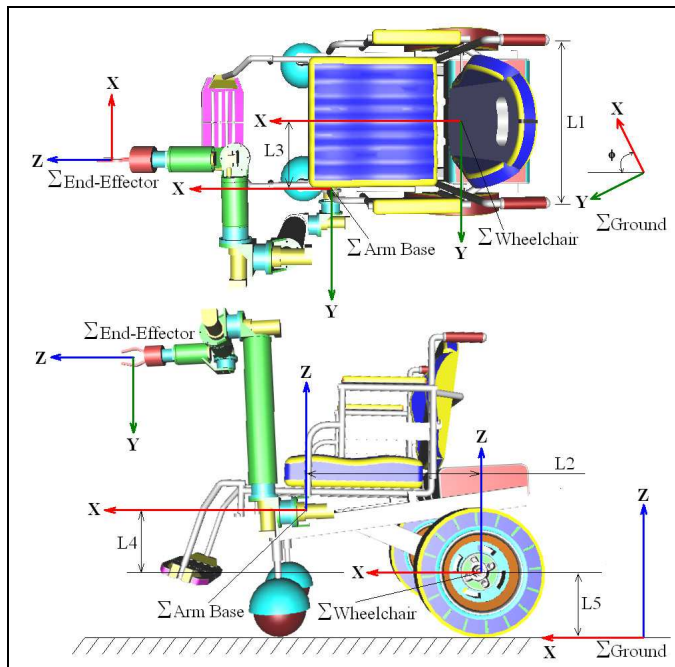

Fig. 4. Coordinate frames and dimensions of interest.

where "P_{xg}" and "P_{yg}" are the x-y coordinates of the end-effector based on the arm base frame, "Φ" is the angle of the arm base frame, which is the same as the angle of the wheelchair based on the ground frame, "L_5" is the wheels' radius, and "L_1" is the distance between the two driving wheels. The above Jacobian can be used to control the wheelchair with the Jacobian of the arm after combining them together.

3.2 The 7-DoF Arm Motion

From the D-H parameters specified in an earlier publication (Alqasemi et al., 2005), the 6x7 Jacobian that relates the joint rates to the Cartesian speeds of the end effector based on the base frame is generated according to Craig's notation (Craig, 2003)

$$\dot{r} = J_A \cdot V_A \tag{2}$$

where:

$$\dot{r} = \begin{bmatrix} \dot{x} & \dot{y} & \dot{z} & \dot{\alpha} & \dot{\beta} & \dot{\gamma} \end{bmatrix}^T \text{ is the task vector, and}$$

$$V_A = \begin{bmatrix} \dot{\theta}_1 & \dot{\theta}_2 & \dot{\theta}_3 & \dot{\theta}_4 & \dot{\theta}_5 & \dot{\theta}_6 & \dot{\theta}_7 \end{bmatrix}^T \text{ is the joint rate vector.}$$

Numerical solutions are implemented using the Jacobian to follow the user directional motion commands or to follow the desired trajectory. Manipulability measure (Yoshikawa, 1990) is used as a factor to measure how far is the current configuration from singularity. This measure is defined as:

$$w = \sqrt{\det(J_A * J_A^T)} \tag{3}$$

Redundancy is resolved in the program structure using Pseudo Inverse of the Jacobian (Yoshikawa, 1990), and singularity is avoided by maximizing the manipulability measure. Since this method carries a guaranteed valid solution only at a singular configuration and not around it, the results carried high joint velocities when singularity is approached. We then decided to use S-R Inverse of the Jacobian (Nakamura, 1991) to give a better approximation around singularities, and use the optimization for different subtasks. S-R Inverse of the Jacobian is used to carry out the inverse kinematics as follows:

$$J_A^* = J_A^T * (J_A * J_A^T + k * I_6)^{-1} \tag{4}$$

where "I_6" is a 6x6 identity matrix, and "k" is a scale factor. It has been known that this method reduces the joint velocities near singularities, but compromises the accuracy of the solution by increasing the joint velocities error. Choosing the scale factor "k" is critical to minimizing the error. Since the point in using this factor is to give approximate solution near and at singularities, an adaptive scale factor is updated at every time step to put the proper factor as needed:

$$k = \begin{cases} k_0 * (1 - \dfrac{w}{w_0})^2 & for \quad w < w_0 \\ 0 & for \quad w \geq w_0 \end{cases}, \tag{5}$$

where "w_0" is the manipulability measure at the start of the boundary chosen when singularity is approached, and "k_0" is the scale factor at singularity. It was found that the optimum values of "w_0" and "k_0" for our system are 20×10^{-3} and 0.35×10^{-3} respectively. Now that the singularity is taken care of using the S-R Inverse of the Jacobian, we can use the joint redundancy to optimize for a secondary task as follows:

$$V_d = J_A^* * \dot{r}_d + (I_7 - J_A^* * J_A) * f \tag{6}$$

where "f" is a 7x1 vector representing the secondary task. That task can either be the desired trajectory in the case of pre-set task execution, or it can be a criterion function that represents the potential energy to be minimized.

3.3 The 9-DoF WMRA System Motion

Combining the two subsystems together by means of Jacobian augmentation (Luca et al., 2006) can give the flexibility of using conventional control and optimization methods without compromising the total system coordinated control. In the case of combined control, let the task vector be:

$$r = f(q_c, q_A \tag{7}$$

Differentiating (7) with respect to time gives:

$$\dot{r} = \frac{\partial f}{\partial q_c}V_c + \frac{\partial f}{\partial q_A}V_A = J_c J_W V_c + J_A V_A = \begin{bmatrix} J_c J_W & J_A \end{bmatrix}\begin{bmatrix} V_c \\ V_A \end{bmatrix} \quad \text{or,} \quad \dot{r} = J \cdot V \tag{8}$$

Solving (8) in conventional methods is now possible. Choosing the Projected Gradient method, gives:

$$\begin{bmatrix} V_W \\ V_A \end{bmatrix} = J^* \dot{r} + \left(I - J^* J\right) V_0 \tag{9}$$

where $V_0 = a\nabla_q H(q)$ for conventional arms, and "H(q)" is the optimization criteria y = H(q).

The existence of the mobile platform means that "Vo" may not exist for non holonomic constraint such as that of the wheelchair. To go around this limitation (Luca et al., 2006) proposed the following: Differentiate the optimization criteria function "H" with respect to time as follows:

$$\dot{y} = \dot{H}(q) = \frac{\partial H}{\partial q_c}V_c + \frac{\partial H}{\partial q_A}V_A = \nabla_q^T H\begin{bmatrix} J_W & 0 \\ 0 & I \end{bmatrix}\begin{bmatrix} V_c \\ V_A \end{bmatrix} \tag{10}$$

In this case, the value of "VH" that improves the objective function is:

$$V_H = \pm a\begin{bmatrix} J_W^T & 0 \\ 0 & I \end{bmatrix}\nabla_q H(q) \equiv V_0 \tag{11}$$

and that velocity vector can be used for optimization. This gives a good representation of the arm joints' velocities and the wheels' velocities of the wheelchair.

Weighted Least Norm solution can also be used as proposed by (Chan & Dubey, 1995). In order to put a motion preference of one joint rather than the other (such as the wheelchair wheels and the arm joints), a weighted norm of the joint velocity vector can be defined as:

$$|V|_W = \sqrt{V^T W V} \tag{12}$$

where "W" is a 9X9 symmetric and positive definite weighting matrix, and for simplicity, it can be a diagonal matrix that represent the motion preference of each joint of the system. For the purpose of analysis, the following transformations are introduced:

$$J_W = J W^{-1/2} \text{ and } V_W = W^{-1/2} V \tag{13}$$

From (12) and (13), it can be shown that the weighted least norm solution is:

$$V_W = W^{-1} J^T \left(J W^{-1} J^T \right)^{-1} \dot{r} \tag{14}$$

The above method has been used in simulation of the 9-DoF WMRA system with the nine state variables "Vd" that represent the seven joint velocities of the arm and the two wheels' velocities of the power wheelchair. It was found that the latter two state variables are of limited use since they tend to unnecessarily rotate the wheelchair back and forth during a long forward motion due to their equal weights. Changing the weights of these two variables will only result in a preference of one's motion over the other.

Two new state variables were introduced out of the wheels' velocities, which represent the angular speed of the wheelchair when both wheels run at equal but opposite velocities and the forward speed of the wheelchair when both wheels run at equal velocities as follows:

$$\dot{\phi} = \frac{2 l_5 \dot{\theta}_r}{l_1}, \quad and \quad \dot{X} = l_5 \dot{\theta}_r \tag{15}$$

The combination of the above two variables would be sufficient to describe any forward and rotational motion of the wheelchair. Having these two state variables in vector "V" instead of the wheels' velocities give a greater advantage in controlling the preferred rotation or translation of the wheelchair. The wheelchair's Jacobian in (1) was changed for the new state variables before augmenting it to the arm's Jacobian, and the results were much better in terms of valuable control. The new state variables are:

$$V = \begin{bmatrix} \dot{\theta}_1 & \dot{\theta}_2 & \dot{\theta}_3 & \dot{\theta}_4 & \dot{\theta}_5 & \dot{\theta}_6 & \dot{\theta}_7 & \dot{X} & \dot{\phi} \end{bmatrix}^T \tag{16}$$

Care must be taken when implementing the above change in the controller algorithm since one of the state variables (the forward motion of the wheelchair) carry linear velocity units, which are different from the rest of the state variables, which carry angular velocity units.

3.4 Criterion Function for Joint Limit Avoidance

The criterion function used for optimization can be defined based on the physical joint limits of the WMRA system, and minimizing such a function results in limiting the joint motion to its limit. A mathematical representation of joint limits in robotic manipulators was proposed (Chan & Dubey, 1995) as follows:

$$H(q) = \sum_{i=1}^{7} \frac{1}{4} \cdot \frac{(q_{i,\max} - q_{i,\min})^2}{(q_{i,\max} - q_{i,current}) \cdot (q_{i,current} - q_{i,\min})} \tag{17}$$

where "q_i" is the angle of joint "i". This criterion function becomes "1" when the current joint angle is in the middle of its range, and it becomes "infinity" when the joint reaches either of its limits. Using this optimization function in (14) can be accomplished through the weight matrix used for optimization. Rather than choosing arbitrary weight values for each individual joint based on the user preference only, an additional value can be added to represent the optimization criterion function as follows:

$$W = \begin{bmatrix} w_{1,u} + \left| \dfrac{\partial H(q)}{\partial q_1} \right| & 0 & \cdots & 0 \\ 0 & w_{2,u} + \left| \dfrac{\partial H(q)}{\partial q_2} \right| & \cdots & 0 \\ \vdots & \vdots & \ddots & \vdots \\ 0 & 0 & \cdots & w_{9,u} + \left| \dfrac{\partial H(q)}{\partial q_9} \right| \end{bmatrix} \qquad (18)$$

where "$w_{i,u}$" is the user-defined weight preference to joint "i", and the second term in each element is the gradient projection of the criterion function defined as:

$$\frac{\partial H(q)}{\partial q_i} = \frac{(q_{i,\max} - q_{i,\min})^2 \cdot (2 \cdot q_{i,current} - q_{i,\max} - q_{i,\min})}{4 \cdot (q_{i,\max} - q_{i,current})^2 \cdot (q_{i,current} - q_{i,\min})^2} \qquad (19)$$

When any particular joint is in the middle of the joint range, (19) becomes zero for that joint, and the only weight left is the user defined weight. On the other hand, when any particular joint is at its limit, (19) becomes "infinity", which means that the joint will carry an infinite weight that makes it impossible to move any further. When the user prefers to move the robotic arm with minimal wheelchair motion, heavy weight can be assigned to the two wheelchair state variables. When any of the robotic arm joints gets close to its limit and its weight approaches infinity, the wheelchair's weight will be much less than that of the joint, and hence it will be more free to move than the joint that is close to its limit.

It is important to note two different deficiencies that may lead to unintended operation or "joint lock" when using this method. The first deficiency is that the joint is penalized with higher weight whether it is approaching its limit or getting away from it. This may cause the robotic arm to use the null space inefficiently by preferring to move a joint with heavy weight going towards its limit rather than moving a joint with heavier weight that is moving away from its limit. This problem was eliminated using the first two conditions in (20) on the criterion function to identify the direction of approach (towards or away from) the joint limit. The second deficiency is that the precise joint limit that takes the weight to "infinity" may never be reached, instead, the numerical solution with its relatively coarse step size may jump from a joint value close to the joint limit before it is reached to a joint value close to the joint limit after it is reached. This will result in a heavy weight that will slowly get lower as the joint gets away from the set limit towards its actual limit. If the previous two conditions were applied alone, the result could be a dangerous motion that gives the weight as "$w_{i,u}$" only since the joint is getting away from its limit from inside that limit. This can either break the joint or lock it when it reaches its actual physical limit with the hard stop. To overcome this deficiency, the last two conditions in (20) were imposed on the criterion function to identify whether the joint is within its limit, or the limit is exceeded.

Imposing the above four conditions (see figure 5), on the weight matrix to perform on the optimization criterion gave the control mechanism much better results in terms of joint limit avoidance and user-preferred motion of each individual variable in the joint space The following condition statement summarizes the conditions imposed in the control code:

$$w_i = w_{i,u} + \begin{cases} \left| \dfrac{\partial H(q)}{\partial q_i} \right| & when \quad q_{min} \leq q_i \leq q_{max} \quad \& \quad \Delta \left| \dfrac{\partial H(q)}{\partial q_i} \right| \geq 0 \\[3mm] 0 & when \quad q_{min} \leq q_i \leq q_{max} \quad \& \quad \Delta \dfrac{\partial H(q)}{\partial q_i} \leq 0 \\[3mm] \infty & when \quad q_{min} \geq q_i \geq q_{max} \quad \& \quad \Delta \dfrac{\partial H(q)}{\partial q_i} \leq 0 \\[3mm] 0 & when \quad q_{min} \geq q_i \geq q_{max} \quad \& \quad \Delta \left| \dfrac{\partial H(q)}{\partial q_i} \right| \geq 0 \end{cases} \qquad (20)$$

Two different trajectory generation functions were implemented in the control system when autonomous operation option was chosen: linear trajectory and polynomial trajectory with parabolic blending (Craig, 2003). The end point can either be given by the user, or can be obtained from an on-board laser pointer, as shown in Figure 6. Three different control reference frames were programmed so that the user can choose the most suited based on the task at hand: The ground frame for autonomous operation with pre-set tasks; the wheelchair's frame for wheelchair motion in the most part; and the end-effector's frame for teleoperation using the end-effector. The option of controlling the arm alone, the wheelchair alone, or the combined wheelchair and arm together was also programmed for the user's convenience.
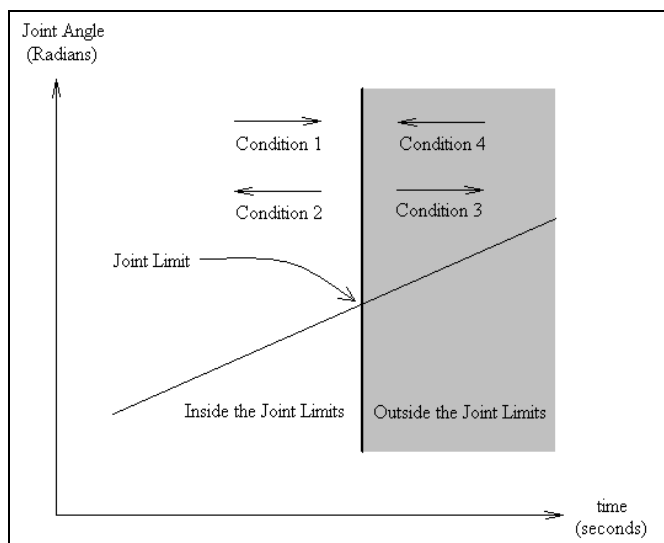

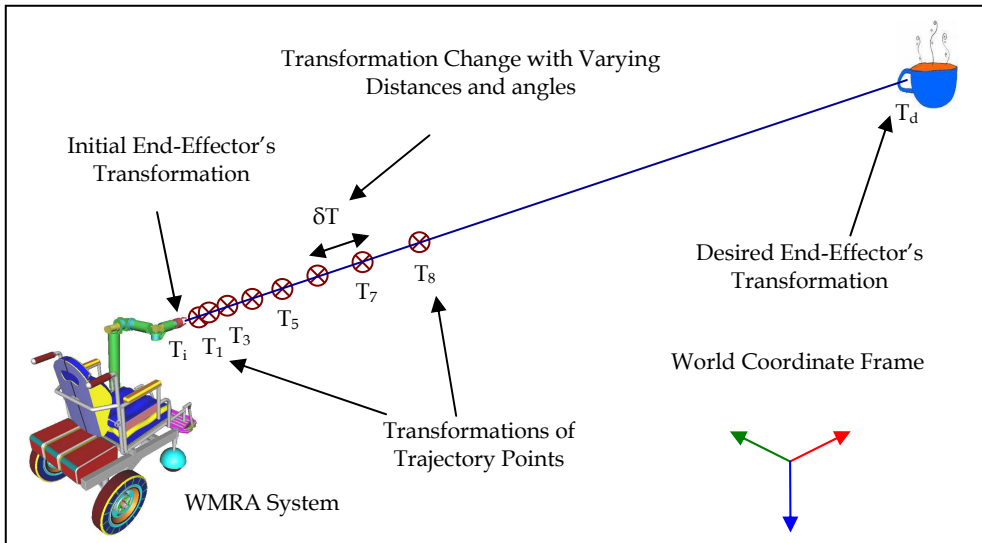Fig. 5. Four joint limit boundary conditions.

Fig. 6. Polynomial trajectory from the gripper to the target.

4. The 9-DoF WMRA System

4.1 Hardware Design of the Arm

An entirely new WMRA was developed, designed and built. The goal was to produce an arm that has better manipulability, greater payload, and easier control than current designs. As found in previous research (Edwards et al., 2006), side mounting is preferable overall because it provides the best balance between manipulability and unobtrusiveness. This mounting location allows the arm to be stowed by folding it back and then wrapping the forearm behind the seat. This helps avoid the stigma that these devices can bring. It virtually disappears when not in use, especially when the arm is painted to match the chair. However, care must be taken to prevent widening of the power chair. Our arm only increases chair width by 7.5cm.

This manipulator is intended for use in Activities of Daily Living (ADL), and for job tasks of a typical office environment. As such, it is important that the arm be strong enough to move objects that are common in these environments. Approximately 4 kg mass is set as the upper limit for a typical around-the-house object that must be manipulated. This was set as the baseline payload for the arm at full horizontal reach at rest. Then, an extra margin of 2 kg was added to allow for a choice of end-effector capable of this load. Reconfigurable arm lengths allow greater leverage on the engineering input, as a single basic design may be adapted to numerous applications. This is only practical with electric drive and actuator placement directly at each joint.
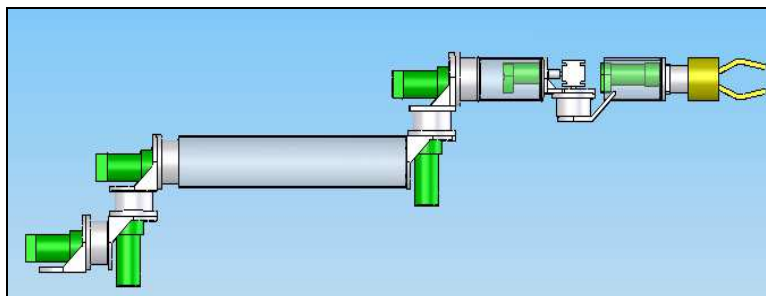
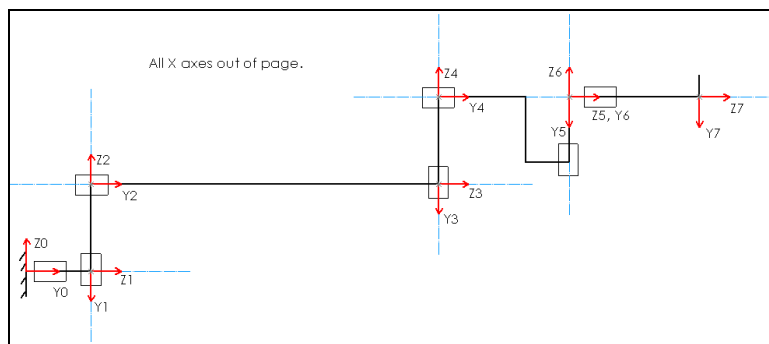Fig. 7. Complete SolidWorks model of the arm.

Fig. 8. Kinematic diagram with link frame assignments.

In the power wheelchair industry, a 24-volt lead-acid battery pack is standard, and is the natural choice for the power supply of a WMRA with minimum power consumption. To have a widespread adoption of these devices, reasonable cost is important. The target was to be in the mid-range of commercially available systems in terms of cost. Extra degrees of freedom help improve manipulability. This is evidenced by the considerable increase going from Raptor's 4 DoF to the 6 DoF of MANUS. Our new design incorporates 7 joints, allowing full pose control even in difficult regions of the workspace, such as reaching around the wheelchair, or up to a high shelf.

The arm is a 7-DoF design, using 7 revolute joints. It is anthropomorphic, with joints 1, 2 and 3 acting as a shoulder, joint 4 as an elbow, and joints 5, 6 and 7 as a wrist as shown in Figure 7. The 3 DoF shoulder allows the elbow to be positioned anywhere along a spherical surface, whereas with the Raptor arm, elbow movement is limited to a circle. Throughout the arm, adjacent joint axes are oriented at 90 degrees as shown in Figure 8. This helps to meet two goals: mechanical design simplicity and kinematic simplicity with low computational cost. All adjacent joint axes intersect, also simplifying the kinematics. The basic arrangement for each joint is a high-reduction gearhead, a motor with encoder and spur-gear reduction, and a bracket that holds these two parts and attaches to the two neighbouring links.

4.2 Hardware Design of the Controller

As shown in Fig 9, PIC-SERVO SC controllers (C1 through C7) that support the DC servo actuators (J1 through J7) were chosen. At 5cm x 7.5cm, this unit has a microprocessor that

drives the built-in amplifier with a PWM signal, handles PID position / velocity control, communicates with RS-485, and can be daisy-chained with up to 32 units. It also reads encoders, limit switches, an 8 bit analogue input, and supports coordinated motion control. Data for the entire arm is interfaced to the main computer using a single serial link. The PIC-Servo SC controllers use RS-485, and a hardware converter interfaces this with the RS-232 or a USB port on the host PC. A timer has been utilized to cut the arm's power off after a preset time to minimize power consumption while not in use. An emergency stop button is placed to cut the power off the motors and leave the logic power on so that the system can be diagnosed without rebooting.

The current host PC is an IBM laptop, running Windows XP. However, the communications protocol is simple and open, and could be adapted to virtually any hardware/software platform with an RS-232 or USB port. Currently, the tested user interfaces are the keyboard and a SpaceBall controller.

4.3 Wheelchair Modification

Figure 10 shows the WMRA system installed on the modified wheelchair "Action Ranger X Storm Series". The wheelchair has been modified by adding an incremental encoder on each one of the wheels. The controller module of the wheelchair has also been modified using TTL compatible signal conditioner and a DA converter so that the signal going to the wheels can be controlled using the same PIC-Servo SC controllers used in the arm. The only difference is that the output from this control board used for the wheelchair is the PWM signal rather than the amplified analogue signal. Two more PIC-Servo SC controllers were added to the control system shown in Figure 9 to control the wheelchair.
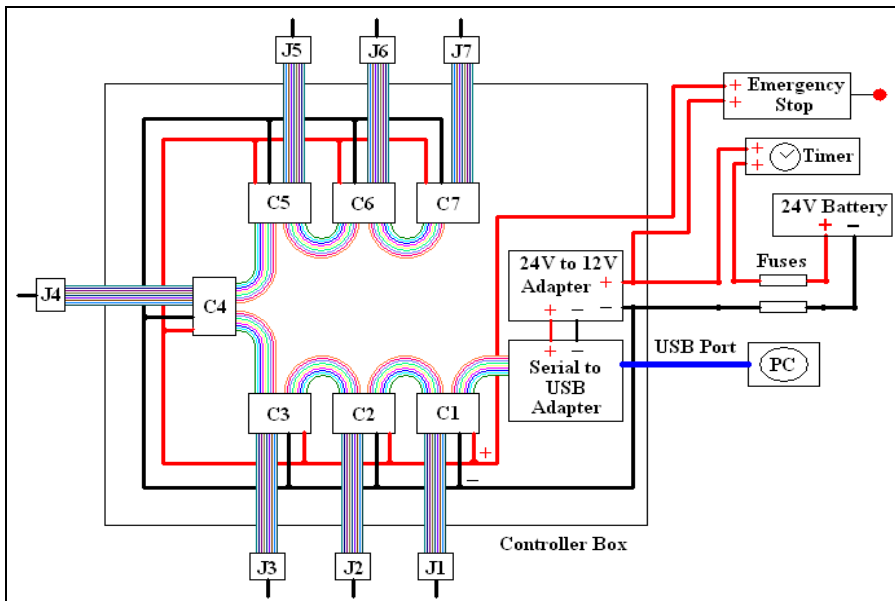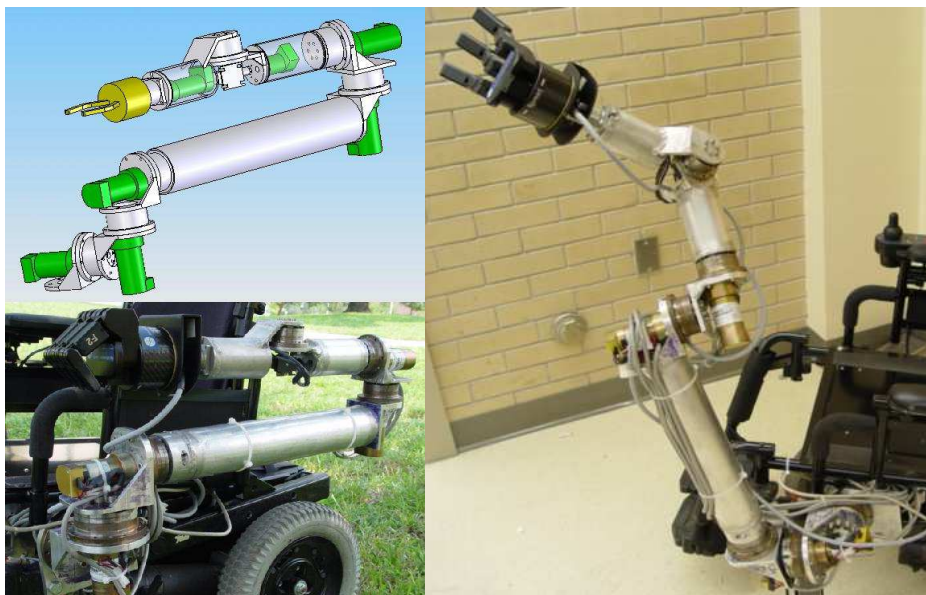

Fig. 9. Control system circuitry of the arm.

Fig. 10. WMRA SolidWorks models and the built device.

4.4 Hardware Design of an Ergonomic Gripper

A new robotic gripper was designed and constructed (Alqasemi et al., 2007) for Activities of
Daily Living (ADL) to be used with the new WMRA. As shown if Figure 11, two aspects of
the new gripper made it unique; one is the design of the paddles, and the other is the design
of the actuation mechanism that produces parallel motion for effective gripping. The
paddles of the gripper were designed to grasp a wide variety of objects with different
shapes and sizes that are used in every day life as shown in Figure 12. The driving
mechanism was designed to be simple, light, effective, safe, self content, and independent of
the robotic arm attached to it.

Fig. 12. Using the new gripper in typical ADL tasks.
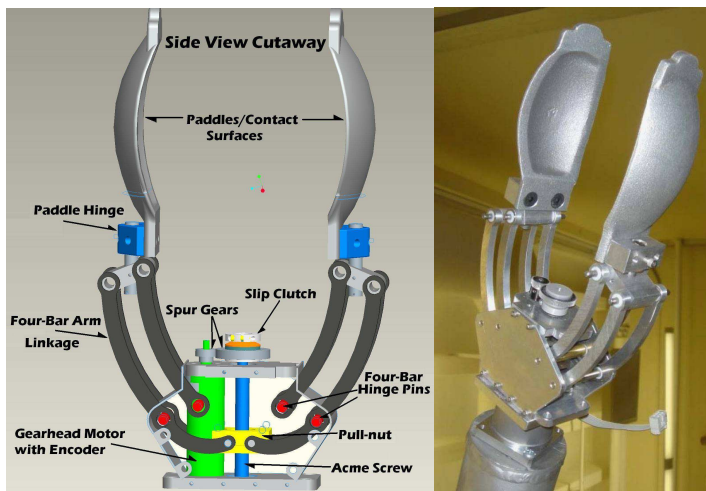
Fig. 11. The designed ergonomic gripper.

4.5 Simulation of the WMRA System in Virtual Reality

The control methods that combined the manipulation and mobility of the newly developed WMRA were tested in simulation before applying them to the actual WMRA system. This step is very important for debugging and inspecting the methods before applying them into the actual arm so that no harm to the physical system is done in case of unexpected errors. In the control software, several options were made available to include the modularity, re-configurability and flexibility requirements for this WMRA system.

The control system was implemented in simulation using Matlab 2008 with Virtual Reality toolbox installed on a PC running Windows XP. Modules of small programs were generated for different operations and different user interfaces, and a main program that uses the modules was developed to simulate the WMRA system using different control parameters and user interfaces, including a Graphical User Interface (GUI). Figure 13 shows a sample of the Virtual Reality simulation.

Fig. 13. Sample of the virtual reality simulation at the initial position.

5. The Integration of the Brain-Computer Interface

In the program structure, flexibility was one of the objectives in the design of user interfaces so that a wider range of these interfaces can be used based on the user's abilities and preference. A six-axis, twelve-way SpaceBall that is capable of moving in the six Cartesian coordinates was implemented. A computer keyboard and a mouse was also used with the on-screen graphical user interface. A touch screen with a choice of robotic actions was programmed as one of the integrated interfaces to the system. Figure 14 shows some of the user interface device options used in the system.

Another user interface used in this work is the Brain-Computer Interface (BCI). Over the past two decades, a variety of studies have evaluated the possibility that brain signals recorded from the scalp or from within the brain could provide new augmentative technology that does not require muscle control (Schalk et al., 2004).

Fig. 14. User interfaces, left to right: SpaceBall, touch screen and GUI.

These BCI systems measure specific features of brain activity and translate them into device control signals as shown in Figure 15. This brain activity can be elicited using a framework called the "oddball paradigm". Studies have shown that when subjects are assigned a task of categorizing an item into 2 possible categories, and one of the two categories occurs infrequently, those events in that rare category will elicit an event-related brain potential (ERP) with latency of about 300 ms, labeled the P300 (Farwell & Donchin, 1988). The P300 is a neural evoked potential component of the EEG, or electroencephalogram (Sutton et al., 1965). It is supposed to follow unexpected sensory stimuli that provide useful information to the subjects according to his/her task. For easier, non-invasive use of this neuro-imaging technology, the user wears a head cap fitted with several electrodes to measure the P300 EEG signals from the activities of the brain.

In this work, the subjects viewed a 5x3 matrix whose rows and columns intensify randomly. Each of the 15 symbols in the matrix corresponds to a specific direction or task command as shown in Figures 15&16. The subject focuses attention on the desired cell carrying his/her desired task or direction of motion. Every time the user counts one more view of the symbol, the P300 EEG signal is recorded, and the corresponding row or column that was shown at that moment was also recorded. In about 15 seconds, the BCI gives the selected row and column of the matrix on the screen as only the row and column containing target cell elicit a P300. The system then translates the chosen character to a corresponding command, which translates into a Cartesian velocity in the proper direction and executes the algorithm to move the arm. As the detection of P300 requires signal averaging, number of trials is required by the system to correctly determine user's intention. The speed of the system thus depends on the number of sequences of flashes required to achieve a given level of accuracy.
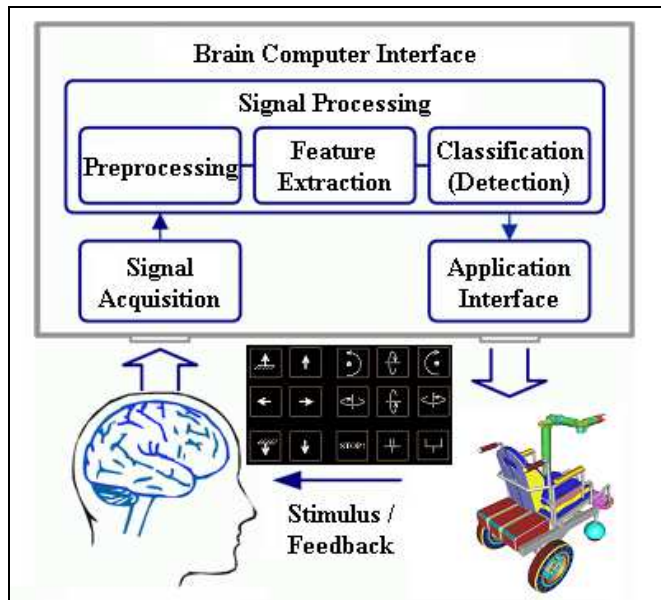
Fig. 15. Basic design and operation of the BCI system.

Fig. 16. WMRA user with BCI electrode cap.

Six able-bodied young adults were able to control the WMRA system movements using the BCI. Participants sat on the wheelchair, wearing a 16-channel electrode cap (Electro Cap International, Inc.) and attended to different symbols on the screen. Every 50 ms a row or a column intensified for 75 ms. For a 5x3 matrix, each sequence of flashes contained 8 intensifications (5 columns and 3 rows) and lasted for 1000 ms. The BCI was also trained to be optimized for each particular human subject, and it showed high accuracy of the selected choice (ranging from 92% to 100 %). These gains were recorded and used for the actual test. We tested the accuracy of character selection as a function of number of sequences of flashes. During the testing phase, a successful control with high accuracy of the motion response was apparent.

6. Experimental Results

The control method used in this work to combine mobility and manipulation in redundant mobile robots was tested using the developed Matlab program that can simulate the WMRA motion and control the physical WMRA system with various user interfaces. The WMRA was commanded to go in an autonomous mode from its default initial position shown in Figure 17 to a defined point in space for the end effector. Several methods were tested in this simulation. In this paper, we will limit our findings to the Weighted Least Norm solution control, and we will discuss the system response using different control methods in an extreme case where the arm was commanded to go to an out-of-reach position.

6.1 Simulation Results Using Different Weights
Three different values were tried for the diagonal elements of the weight matrix "W_d" to implement the control system and to verify its effectiveness in damping the wheelchair motion or the arm motion. Figures 18 through 20 show the final poses of the WMRA system after the end-effector reached the desired destination for the five cases studied.

Fig. 17. Initial WMRA pose.

Fig. 18. Destination pose - Wd = [1, 1, 1, 1, 1, 1, 1, 1, 1].

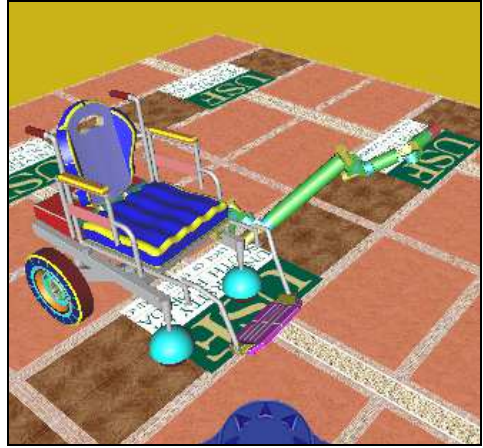Fig. 19. Destination pose - *Wd* = [10, 10, 10, 10, 10, 10, 10, 1, 1].

Fig. 20. Destination pose - *Wd* = [1, 1, 1, 1, 1, 1, 1, 100, 100].

The weight matrix of the first case carried in its diagonal elements "1" for each of the arm's seven joints, and "1" for wheelchair's position and orientation variables, which means that the wheelchair's two variables and the arm's joints carry the same tendency for motion, as shown in Figure 18. In this case, the weight matrix is useless since it is identity. The weight matrix of the second case carried in its diagonal elements "10" for each of the arm's seven joints, and "1" for wheelchair's position and orientation variables, which means that the wheelchair's two variables are 10 times more likely to move than the arm's joints, and that is apparent in the results shown in Figure 19. In the third case, "W_d" carried weights of "1" for the arm's seven joints, and a weight of "100" for the wheelchair's position and orientation. This means that the arm's joints are 100 times more likely to move than the wheelchair's two variables, and Figure 20 shows how the wheelchair's motion was minimal.

The simulation program was designed to give different useful values and plots throughout the simulation process for observation and diagnosis of any potential problems that might occur during the task execution. In the first case, when all 9 variables carried the same weights, an apparent motion in the arm and the wheelchair alike occurred. In the second case, when the arm carried a heavy weight in the weight matrix, it was clear that the seven arm joints had minimal motion that was necessary for the destination to be reached. That end-effector destination was impossible to reach by using the two wheelchair's variables only. The third case shows an easy arm motion and very minimal wheelchair motion that was necessary to avoid singularity.

An important property of this optimization method was apparent during simulation, which was the minimization of singularity. As the arm was moving to the destination and both wheels were moving backwards, the wheels reversed their motion in the middle of the simulation period when the arm started approaching singularity. Figures 21 through 23 show the manipulability index of both arm only and the combined WMRA system. It is important to note here that these values were multiplied by (10^{-9}) to get the normalized manipulability measure. It is clear that the manipulability is much higher for the WMRA

system than that of the arm only due to the fact that the WMRA system carries two more degrees of freedom.
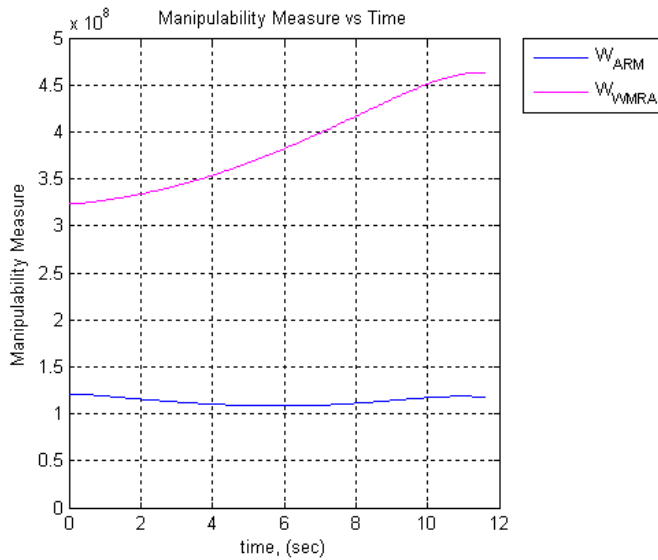

Fig. 21. Manipulability index - *Wd* = [1, 1, 1, 1, 1, 1, 1, 1, 1].
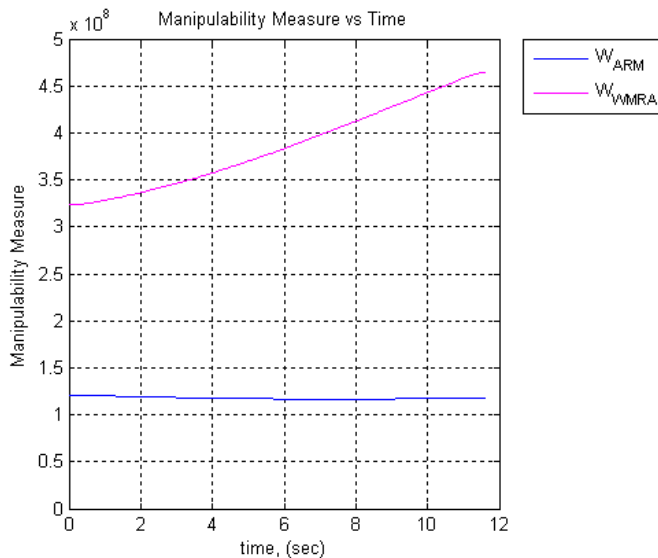

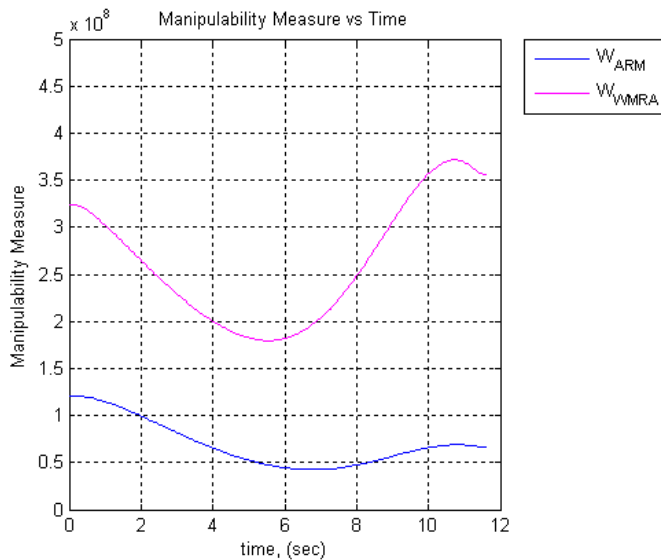Fig. 22. Manipulability index - *Wd* = [10, 10, 10, 10, 10, 10, 10, 1, 1].

Fig. 23. Manipulability index - Wd = [1, 1, 1, 1, 1, 1, 1, 100, 100].

In all three cases, the manipulability measure was maximized based on the weight matrix. Figure 21 shows an improvement trend of the WMRA's manipulability index over the arm's manipulability index towards the end of simulation. Figure 22 shows the manipulability of the arm as nearly constant compared to that in Figure 23 because of the minimal motion of the arm. Figure 23 shows how the wheelchair started moving rapidly later in the simulation (see figure 20) as the arm approached singularity, even though the weight of the wheelchair motion was heavy. This helped in improving the WMRA system's manipulability.

6.2 Simulation Results in an Extreme Case

To test the difference in the system response when using different methods, an extreme case was tested, where the WMRA system is commanded to reach a point that is physically unreachable. The end-effector was commanded to move horizontally and vertically upwards to a height of 1.3 meters from the ground, which is physically unreachable, and the WMRA system will reach singularity. The response of the system can avoid that singularity depending on the method used. Singularity, joint limits and preferred joint-space weights were the three factors we focused on in this part of the simulation. Eight control cases simulated were as follows:

(a) Case I: Pseudo inverse solution (PI): In this case, the system was unstable, the joints went out of bounds, and the user had no weight assignment choice.

(b) Case II: Pseudo inverse solution with the gradient projection term for joint limit avoidance (PI-JL): In this case, the system was unstable, the joints stayed in bounds, and the user had no weight assignment choice.

(c) Case III: Weighted Pseudo inverse solution (WPI): In this case, the system was unstable, the joints went out of bounds, and the user had weight assignment choices.

(d) Case IV: Weighted Pseudo inverse solution with joint limit avoidance (WPI-JL): In this case, the system was unstable, the joints stayed in bounds, and the user had weight assignment choices.

(e) Case V: S-R inverse solution (SRI): In this case, the system was stable, the joints went out of bounds, and the user had no weight assignment choice.

(f) Case VI: S-R inverse solution with the gradient projection term for joint limit avoidance (SRI-JL): In this case, the system was unstable, the joints stayed in bounds, and the user had no weight assignment choice.

(g) Case VII: Weighted S-R inverse solution (WSRI): In this case, the system was stable, the joints went out of bounds, and the user had weight assignment choices.

(h) Case VIII: Weighted S-R inverse solution with joint limit avoidance (WSRI-JL): In this case, the system was stable, the joints stayed in bounds, and the user had weight assignment choices.

In the first case, Pseudo inverse was used in the inverse Kinematics without integrating the weight matrix or the gradient projection term for joint limit avoidance. Figure 24 shows how this conventional method led to the singularity of both the arm and the WMRA system. The user's preference of weight was not addressed, and the joint limits were discarded. In the last case, the developed method that uses weighted S-R inverse and integrates the gradient projection term for joint limit avoidance was used in the inverse kinematics. Figure 25 shows the best performance of all tested methods since it fulfilled all the important control requirements. This last method avoided singularities while keeping the joint limits within bounds and satisfying the user-specified weights as much as possible. The desired trajectory was followed until the arm reached its maximum reach perpendicular to the ground. Then it started pointing towards the current desired trajectory point, which minimizes the position errors. Note that the arm reaches the minimum allowed manipulability index, but when combined with the wheelchair, that index stays farther from singularity.
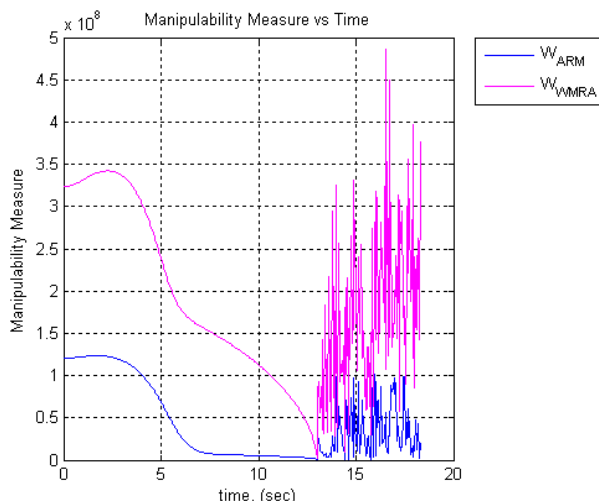

Fig. 24. Manipulability index – using only Pseudo inverse in an extreme case.

It is important to mention that changing the weights of each of the state variables gives motion priority to these variables, but may lead to singularity if heavy weights are given to certain variables when they are necessary for particular motions. For example, when the seven joints of the arm were given a weight of "1000" and the task required rapid motion of the arm, singularity occurred since the joints were nearly stationary. Changing these weights dynamically in the control loop depending on the task in hand leads to a better performance. This subject will be explored and published in a later publication.
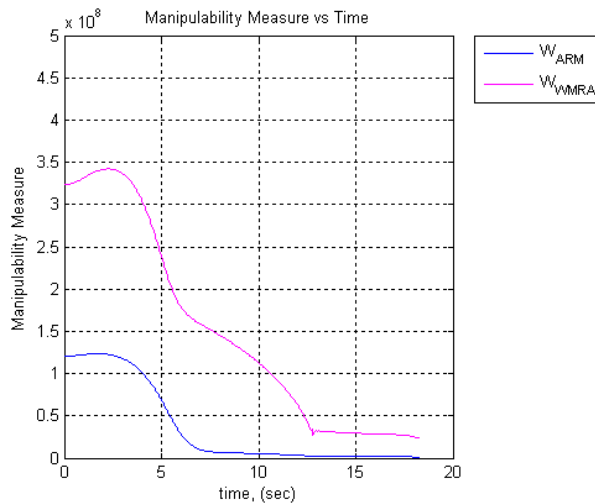
Fig. 25. Manipulability index – using weighted S-R inverse with the gradient projection term for joint limit avoidance in an extreme case.

6.3 Clinical Testing on Human Subjects

In the teleoperation mode of the testing, several user interfaces were tested. Figure 29 shows the WMRA system with the Barrette hand installed and a video camera used by a person affected by Guillain-Barre Syndrome. In her case, she was able to use both the computer interface and the touch-screen interface. Other user interfaces were tested, but in this paper, we will discuss the BCI user interface results. When asked, participants informed the tester that they preferred the 4 and 6 sequences of flashes over the longer sequences. The common explanation was that it was easier to stay focused for shorter periods of time. Figure 30 shows accuracy data obtained when participants spelled 50 characters of each set of sequences (12, 10, 8, 6, 4, and 2). As the number of sequences of flashes decrease, the speed of the BCI system increases as the maximum number of characters read per unit of time increases. This compromise affects the accuracy of the selected characters. Figure 31 shows the mean percentages correct for each of the sequences. The percentages are presented as number of maximum characters per minute.

The results call for the evaluation of the speed accuracy trade-off in an online mode rather than in an offline analysis to account for the users' ability to attend to a character over time. Few potential problems were noticed as follows: Every full scan of a single user input takes about 15 second, and that might cause a delay in the response of the WMRA system to

change direction on time as the human user wishes. This 15-second delay may cause problems in case the operator needs to stop the WMRA system for a dangerous situation such as approaching stairs, or if the user made the wrong selection and needed to return back to his original choice.

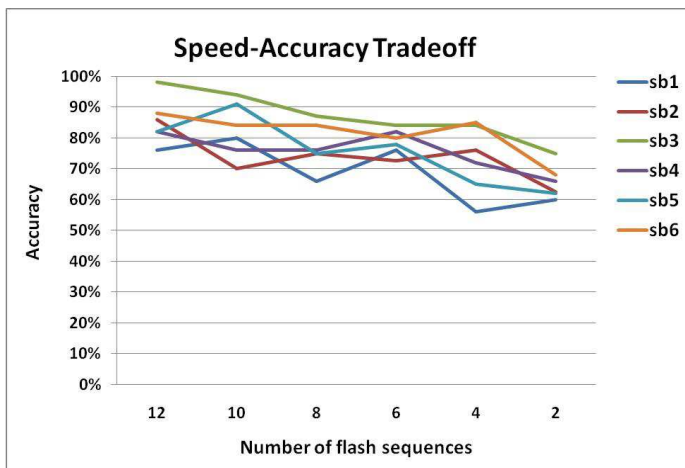Fig. 29. A person with Guillain-Barre Syndrome driving the WMRA system.
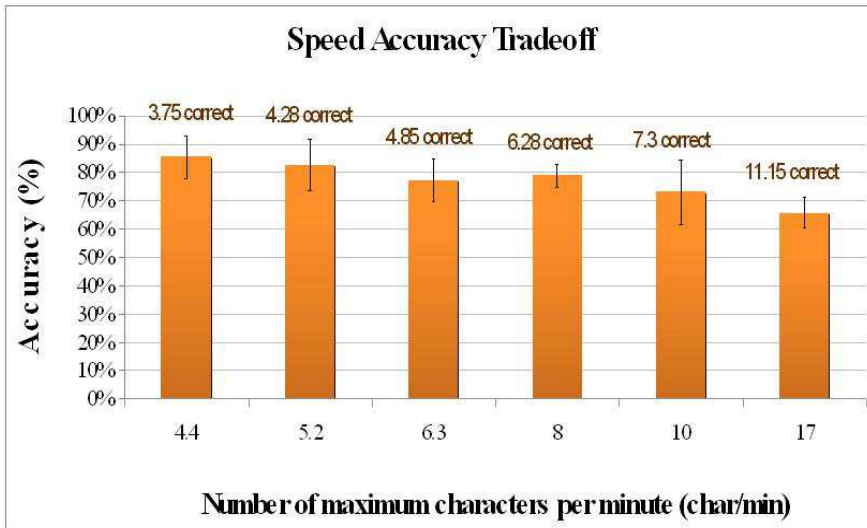

Fig. 30. Accuracy data (% correct) for 6 human subjects.

Fig. 31. Accuracy data (% correct) for each of the flash sequences.

It is also noted that after an extended period of time in using the BCI system, fatigue starts to appear on the user due to his concentration on the screen when counting the appearances of his chosen symbol. This tiredness on the user's side can be a potential problem.

Furthermore, when the user needs to constantly look at the screen and concentrate on the chosen symbol, This will distract him from looking at where the WMRA is going, and that poses some danger on the user. Despite the above noted problems, a successful interface with a good potential for a novel application was developed. Further refinement of the BCI interface is needed to minimize potential risks.

7. Conclusions and Recommendations

A wheelchair-mounted robotic arm (WMRA) was designed and built to meet the needs of mobility-impaired persons, and to exceed the capabilities of current devices of this type. Combining the wheelchair control and the arm control through the augmentation of the Jacobian to include representations of both resulted in a control system that effectively and simultaneously controls both devices at once. The control system was designed for coordinated Cartesian control with singularity robustness and task-optimized combined mobility and manipulation. Weighted Least Norm solution was implemented to prioritize the motion between different arm joints and the wheelchair.

Modularity in both the hardware and software levels allowed multiple input devices to be used to control the system, including the Brain-Computer Interface (BCI). The ability to communicate a chosen character from the BCI to the controller of the WMRA was presented, and the user was able to control the motion of WMRA system by focusing attention on a specific character on the screen. Further testing of different types of displays (e.g. commands, picture of objects, and a menu display with objects, tasks and locations) is planned to facilitate communication, mobility and manipulation for people with severe

disabilities. Testing of the control system was conducted in Virtual Reality environment as well as using the actual hardware developed earlier. The results were presented and discussed.

8. References

Alqasemi, R.; Mahler, S.; Dubey, R. (2007). "Design and construction of a robotic gripper for activities of daily living for people with disabilities," Proceedings of the 2007 ICORR, Noordwijk, the Netherlands, June 13–15.

Alqasemi, R.M.; McCaffrey, E.J.; Edwards, K.D. and Dubey, R.V. (2005). "Analysis, evaluation and development of wheelchair-mounted robotic arms," Proceedings of the 2005 ICORR, Chicago, IL, USA.

Chan, T.F.; Dubey, R.V. (1995). "A weighted least-norm solution based scheme for avoiding joint limits for redundant joint manipulators," IEEE Robotics and Automation Transactions (R&A Transactions 1995). Vol. 11, Issue 2, pp. 286-292.

Chung, J.; Velinsky, S. (1999). "Robust interaction control of a mobile manipulator - dynamic model based coordination," Journal of Intelligent and Robotic Systems, Vol. 26, No. 1, pp. 47-63.

Craig, J. (2003). "Introduction to robotics mechanics and control," Third edition, Addison-Wesley Publishing, ISBN 0201543613.

Edwards, K.; Alqasemi, R.; Dubey, R. (2006). "Design, construction and testing of a wheelchair-mounted robotic arm," Proceedings of the 2006 ICRA, Orlando, FL, USA.

Eftring, H.; Boschian, K. (1999). "Technical results from manus user trials," Proceedings of the 1999 ICORR, 136-141.

Farwell, L.; Donchin, E. (1988). "Talking off the top of your head: Toward a mental prosthesis utilizing event-related brain potentials," Electroencephalography and Clinical Neurophysiology, 70, 510–523.

Galicki, M. (2005). "Control-based solution to inverse kinematics for mobile manipulators using penalty functions," 2005 Journal of Intelligent and Robotic Systems, Vol. 42, No. 3, pp. 213-238.

Luca, A.; Oriolo, G.; Giordano, P. (2006). "Kinematic modeling and redundancy resolution for nonholonomic mobile manipulators," Proceedings of the 2006 ICRA, pp. 1867-1873.

Lüth, T.; Ojdaniæ, D.; Friman, O.; Prenzel, O.; and Gräser, A. (2007). "Low level control in a semi-autonomous rehabilitation robotic system via a Brain-Computer Interface," Proceedings of the 2007 ICORR, Noordwijk, The Netherlands.

Mahoney, R. M. (2001). "The Raptor wheelchair robot system", Integration of Assistive Technology in the Information Age. pp. 135-141, IOS, Netherlands.

Nakamura, Y. (1991). "Advanced robotics: redundancy and optimisation," Addison- Wesley Publishing, ISBN 0201151987.

Papadopoulos, E.; Poulakakis, J. (2000). "Planning and model-based control for mobile manipulators," Proceedings of the 2001 IROS.

Reswick, J.B. (1990). "The moon over dubrovnik - a tale of worldwide impact on persons with disabilities," Advances in External Control of Human Extremities.

Schalk, G.; McFarland, D.; Hinterberger, T.; Birbaumer, N.; and Wolpaw, J. (2004). "BCI2000: A general-purpose brain-computer interface (BCI) system," IEEE Transactions on Biomedical Engineering, V. 51, N. 6, pp. 1034-1043.

Sutton, S.; Braren, M.; Zublin, J. and John, E. (1965). "Evoked potential correlates of stimulus uncertainty," Science, V. 150, pp. 1187–1188.

US Census Bureau, "Americans with disabilities: 2002," Census Brief, May 2006, http://www.census.gov/prod/2006pubs/p70-107.pdf

Valbuena, D.; Cyriacks, M.; Friman, O.; Volosyak, I.; and Gräser, A. (2007). "Brain-computer interface for high-level control of rehabilitation robotic systems," Proceedings of the 2007 ICORR, Noordwijk, The Netherlands.

Yanco, Holly (1998). "Integrating robotic research: a survey of robotic wheelchair development," AAAI Spring Symposium on Integrating Robotic Research, Stanford, California.

Yoshikawa, T. (1990). "Foundations of robotics: analysis and control," MIT Press, ISBN 0262240289.

Advances in Robot Manipulators
Edited by Ernest Hall

The purpose of this volume is to encourage and inspire the continual invention of robot manipulators for science and the good of humanity. The concepts of artificial intelligence combined with the engineering and technology of feedback control, have great potential for new, useful and exciting machines. The concept of eclecticism for the design, development, simulation and implementation of a real time controller for an intelligent, vision guided robots is now being explored. The dream of an eclectic perceptual, creative controller that can select its own tasks and perform autonomous operations with reliability and dependability is starting to evolve. We have not yet reached this stage but a careful study of the contents will start one on the exciting journey that could lead to many inventions and successful solutions.

How to reference
In order to correctly reference this scholarly work, feel free to copy and paste the following:

Redwan Alqasemi and Rajiv Dubey (2010). A 9-DoF Wheelchair-Mounted Robotic Arm System: Design, Control, Brain-Computer Interfacing, and Testing, Advances in Robot Manipulators, Ernest Hall (Ed.), ISBN: 978-953-307-070-4, InTech, Available from: http://www.intechopen.com/books/advances-in-robot-manipulators/a-9-dof-wheelchair-mounted-robotic-arm-system-design-control-brain-computer-interfacing-and-testing

INTECH
open science | open minds